17th World Conference on Earthquake Engineering, 17WCEE
Sendai, Japan - September 13th to 18th 2020

Strong Motion Observation at Kanto Gakuin University Kanazawa Hakkei Campus in Yokohama -Vibration Characteristics of the Building No. 5-

H. Watanabe[(1)], K. Chiba[(2)], S. Fukuyama[(3)] and Y. Sano[(4)]

[(1)] *Associate Professor, Kanto Gakuin University, hwatanab@kanto-gakuin.ac.jp*
[(2)] *Bachelor Course Student, Kanto Gakuin University, f16N1079@kanto-gakuin.ac.jp*
[(3)] *Bachelor Course Student, Kanto Gakuin University, f16N1111@kanto-gakuin.ac.jp*
[(4)] *Assistant, Kanto Gakuin University, ysano@kanto-gakuin.ac.jp*

Abstract

Seismic observation has been carried out on a building with an environmental control system (Kanto Gakuin University Kanazawa Hakkei Campus No.5 Building), located in Kanazawa-ward, Yokohama, since 31 March, 2019. The purpose is to contribute to monitoring the structural deterioration with age and the structural changes by experiencing various levels of earthquakes and also giving grounds for discussing the usability of the building if it should experience a massive earthquake. In this study, we report on the vibration characteristics of the Building No. 5, based on the observation records obtained about a year after the start of observation. We also report on the damage to the building based on the predominant period of the Building No. 5 and the principal direction of acceleration in each floor obtained from the earthquake records. The Building No. 5 was completed in June 2014. The structure is made of reinforced concrete (steel reinforced concrete only on the 5th floor) as a rigid framed structure. The building has 5 stories above the ground, and has approximately 44.4m x 16m in plan and 19.53m in height. IT strong motion seismometers are installed on the first, second, third, fourth, fifth floors and top of the building. At the observation point of each strong motion seismometer, two horizontal components (long side direction X, short side direction Y) and vertical component (vertical direction Z) are measured. The target earthquakes were observed by the IT strong motion seismometer in the Building No. 5 for about a year since the start of observation on 31 March, 2019. The vibration characteristics of the Building No. 5 were examined using the observation record on 24 June, 2019, when the largest seismic intensity was observed in Kanazawa-ward, Yokohama. The predominant period was seen at 0.325 s (3.08 Hz) in the long side direction and 0.306 s (3.27 Hz) in the short side direction. Although there was some variation in the long side direction and the short side direction, the predominant period in the long side direction was distributed in the vicinity of 0.321 s from the start of observation and showed an almost constant value. Similarly, the predominant period in the short side direction was distributed around 0.295s, and there was almost no change in the predominant period of the Building No. 5.

Compared to the other buildings with same height, the Building No.5 has a shorter natural period. The change in the predominant period was not as great as the change in the period corresponding to the change in stiffness when the columns on the first floor reached yield. The apparent torsion angle per unit length based on the principal axis of acceleration of each floor was distributed within 0.103rad./m.

Keywords: seismic observation; predominant period; apparent angle of twist per unit of length

1. Introduction

Seismic observation has been carried out on a medium-rise reinforced concrete building (Kanto Gakuin University Kanazawa Hakkei Campus Building No.5), located at Kanazawa-ward, Yokohama, since 31 March, 2019. The purpose is to contribute to monitoring the structural deterioration with age and the structural changes by experiencing various levels of earthquakes and also giving grounds for discussing the usability of the building if it should experience a massive earthquake.
Ota and others (2016, 2017 and 2018) made a report on the dynamic characteristics of another building which could be inferred from the records obtained in the measured record Fubruary, 2015 through January, 2019. In this report, we make use of only the information obtained by the seismometers installed in the building, which was not equipped with the software devised by Kusunoki (2006). And then we will suggest some preparatory criteria evaluate the damage on buildings, showing data from the latest seismic observation.

2. Target building and Observation System

Fig.1 (a) shows the target building, and Table 1 shows its specifications. The building was completed in 2014. The building has 5 stories above the ground, and has approximately 44.4m x 16m in plan and 19.53m in height.

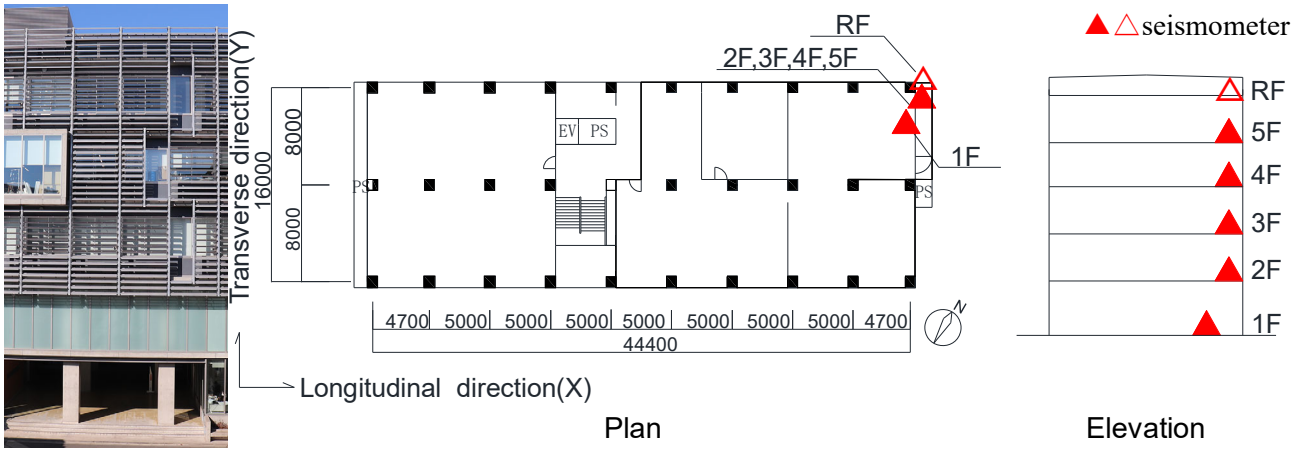

(a)south view of building No.5 (b)layout of measuring equipment

Fig.1 – Outline of the building and layout of the seismometers

Table 1 – Specification of the building

Location	Kanazawa-ward, Yokohama, Japan
Main uses	School Building of University
Number of stories	Five stories above ground, one-story penthouse
Height	23.53 m
Structure	Reinforced concrete / Steel / Steel-framed Reinforced Concrete
Complete	2014

The first horizontal natural period on the building was calculated by using the following method.

a) by using abbreviated equation (1), with H=19.53m

$$T_1 = 0.02H \tag{1}$$

Fig.1 (b) shows the layout of the seismometers. Six IT strong motion seismometers, which were set at 100Hz in three directions, were installed on 1F, 2F, 3F, 4F, 5F, and RF.

Table 2 shows the specifications of the seismometers, Table 3 shows details of the earthquake of seismic intensity 1 or greater measured on the building, and Fig.2 shows the acceleration wave forms obserbed in an earthquake just for an example.

Table 2 Specifications of the seismometers

sampling [Hz]	noise [cm/s/s]	acceleration range [cm/s/s]
100	0.1	±2450

3. Analysis method

In this study, we focus attention on 32 earthquakes of seismic intensity 2 or greater out of the 46 of seismic intensity 1 or greater which had been observed in the building. These Fourier spectra were calculated from the time history data of acceleration. The microtremor is not included in the analysis because the natural period might not be evaluated as a short period. Therefore, the secondary wave only is targeted with the number of data being a power of 2. The secondary wave part was selected visually and the maximum response value was included in the analysis target time, based on the response acceleration time history of the first floor level.

These spectra smoothed with Parzen window at a band width of 0.2Hz in the FFT method. Transfer functions were calculated by using Fourier spectrum ratios based on the first floor. Fig.3 shows Fourier spectrum ratios on RF/1F, 5F/1F, 4F/1F, 3F/1F, and 2F/1F.

The periods were considered on the top floor as a representative in this research. Some peak periods could be seen in the Fourier spectrum ratio. Among the peak periods, the peak period with the largest Fourier spectral ratio value was defined as the predominant period. In Fig. 3, in the X (longitudinal) direction, the dominant period is 0.325 s, and in the Y (transverse) direction, the dominant period is 0.306 s.

The in-torsion angles were considered from the acceleration records on each measurement floor. In Fig. 4, the trajectories of the acceleration in the X (longitudinal) direction and the Y (transverse) direction in the acceleration records are indicated by the black solid line. The numerical lines indicating the trajectories are called as *acceleration orbits*, and the approximate straight lines by using the least squares method are indicated by red numerical lines with respect to the numeric lines in the figure. The approximate lines thus obtained were assumed to be the *principal axes* here. It can be seen that the principal axes are shown mainly along the X (longitudinal) direction. The apparent angle of torsion θ [rad./m] which is per unit length to the bottom floor was obtained by dividing the rotation angle of the principal axis of the upper floor plane with the principal axis of the lower floor plane by the distance between the seismometers.

Table 3 – Details of the earthquake measured on the building

No.	Start Date		Measured seismic intensity of the building (JMA Scale)		Epicenter (JMA)	the north latitude [°] (JMA)	the east longitude [°] (JMA)	focal depth [km] (JMA)
			$_1I_{JMA}$ (in 1st floor)	$_{max}I_{JMA}$ (Max Intensity)				
1	5 April, 2019	17:23:47	1.0	1.56	SE Off Chiba Pref.	34.68	140.12	63
2	5 April, 2019	18:59:21	0.0	1.56	Near Torishima Is.	30.40	139.01	414
3	20 May, 2019	7:49:22	0.5	1.42	SE Off Chiba Pref.	35.00	140.08	17
4	24 May, 2019	12:40:57	0.5	1.24	S Saitama Pref.	35.95	139.41	106
5	25 May, 2019	15:21:06	2.6	3.23	NE Chiba Pref.	35.36	140.29	38
6	1 June, 2019	7:58:31	2.2	2.73	NE Chiba Pref.	35.37	140.29	35
7	4 June, 2019	13:42:17	0.9	1.24	Near Torishima Is.	29.06	139.66	445
8	11 June, 2019	10:59:38	0.6	1.33	NW Chiba Pref.	35.81	140.19	60
9	17 June, 2019	8:00:58	1.4	2.05	N Ibaraki Pref.	36.52	140.58	77
10	18 June, 2019	22:23:37	1.6	1.90	Off Yamagata Pref.	38.61	139.48	14
11	20 June, 2019	1:56:18	1.1	1.78	SE Off Chiba Pref.	35.01	140.20	76
12	24 June, 2019	9:12:01	3.2	3.91	SE Off Chiba Pref.	34.93	139.96	61
13	24 June, 2019	19:23:04	0.6	1.61	E Off Izu Peninsula	35.07	139.10	8
14	7 July, 2019	3:52:35	0.8	1.59	E Off Chiba Pref.	35.65	140.73	48
15	8 July, 2019	19:18:38	0.3	1.40	SE Off Chiba Pref.	34.84	139.98	54
16	8 July, 2019	22:54:44	1.8	2.48	W Kanagawa Pref.	35.51	139.09	23
17	19 July, 2019	14:20:10	0.0	1.03	NW Chiba Pref.	35.62	140.12	68
18	23 July, 2019	15:28:35	0.8	1.86	NW Chiba Pref.	35.64	140.16	67
19	25 July, 2019	7:14:42	1.9	2.38	E Off Chiba Pref.	36.33	140.57	58
20	28 July, 2019	3:32:12	2.7	2.98	SE Off Mie Pref.	33.16	137.40	393
21	30 July, 2019	5:38:29	2.6	3.29	E Off Hachijō-jima Is.	32.91	140.78	59
22	4 August, 2019	19:24:02	3.0	3.59	Off Fukushima Pref.	37.71	141.63	45
23	12 August, 2019	16:39:27	0.2	1.30	SE Off Mie Pref.	34.85	139.86	51
24	23 August, 2019	20:49:54	1.0	2.02	S Chiba Pref.	35.35	140.02	40
25	27 August, 2019	0:13:52	0.8	1.33	W Kanagawa Pref.	35.50	139.07	14
26	14 September, 2019	11:55:01	0.8	1.35	NW Chiba Pref.	35.65	140.17	62
27	6 October, 2019	18:28:33	0.1	1.42	E Off Chiba Pref.	35.20	140.55	59
28	9 October, 2019	4:58:52	0.6	1.63	NW Chiba Pref.	35.80	140.11	62
29	12 October, 2019	18:22:11	2.1	2.73	SE Off Mie Pref.	34.67	140.65	75
30	20 October, 2019	11:20:14	0.3	1.20	E Tama, Tokyo	35.66	139.44	27
31	31 October, 2019	11:06:55	0.1	1.15	NW Chiba Pref.	35.80	140.11	62
32	17 November, 2019	20:05:50	1.8	2.48	Near Izu-oshima Is.	34.64	139.05	13
33	22 November, 2019	5:24:13	1.7	2.21	S Ibaraki Pref.	36.07	139.89	45
34	3 December, 2019	1:18:27	1.6	2.24	S Nagano Pref.	35.80	137.50	8
35	3 December, 2019	20:02:22	0.5	1.62	NW Chiba Pref.	35.73	139.97	78
36	4 December, 2019	10:39:32	1.5	2.19	N Ibaraki Pref.	36.81	140.54	9
37	4 December, 2019	19:35:51	1.4	1.86	N Tochigi Pref.	36.95	139.68	7
38	11 December, 2019	18:40:27	1.0	1.35	Off Fukushima Pref.	37.73	141.80	41
39	14 December, 2019	3:24:09	2.3	2.70	Near Izuoshima Is.	35.03	139.45	33
40	16 December, 2019	4:14:13	0.6	1.61	E Off Chiba Pref.	35.15	140.57	59
41	3 January, 2020	3:24:14	2.2	2.62	E Off Chiba Pref.	35.81	141.12	34
42	14 January, 2020	4:54:06	2.3	2.70	S Ibaraki Pref.	36.08	139.88	46
43	14 January, 2020	13:26:26	0.6	1.19	Off Ibaraki Pref.	36.12	140.88	52
44	1, February, 2020	1:11:40	1.7	2.24	E Off Chiba Pref.	35.67	140.71	50
45	1, February, 2020	2:08:00	2.6	3.10	S Ibaraki Pref.	35.97	140.06	63
46	6, February, 2020	20:20:39	1.4	1.73	Off Ibaraki Pref.	36.34	141.73	54

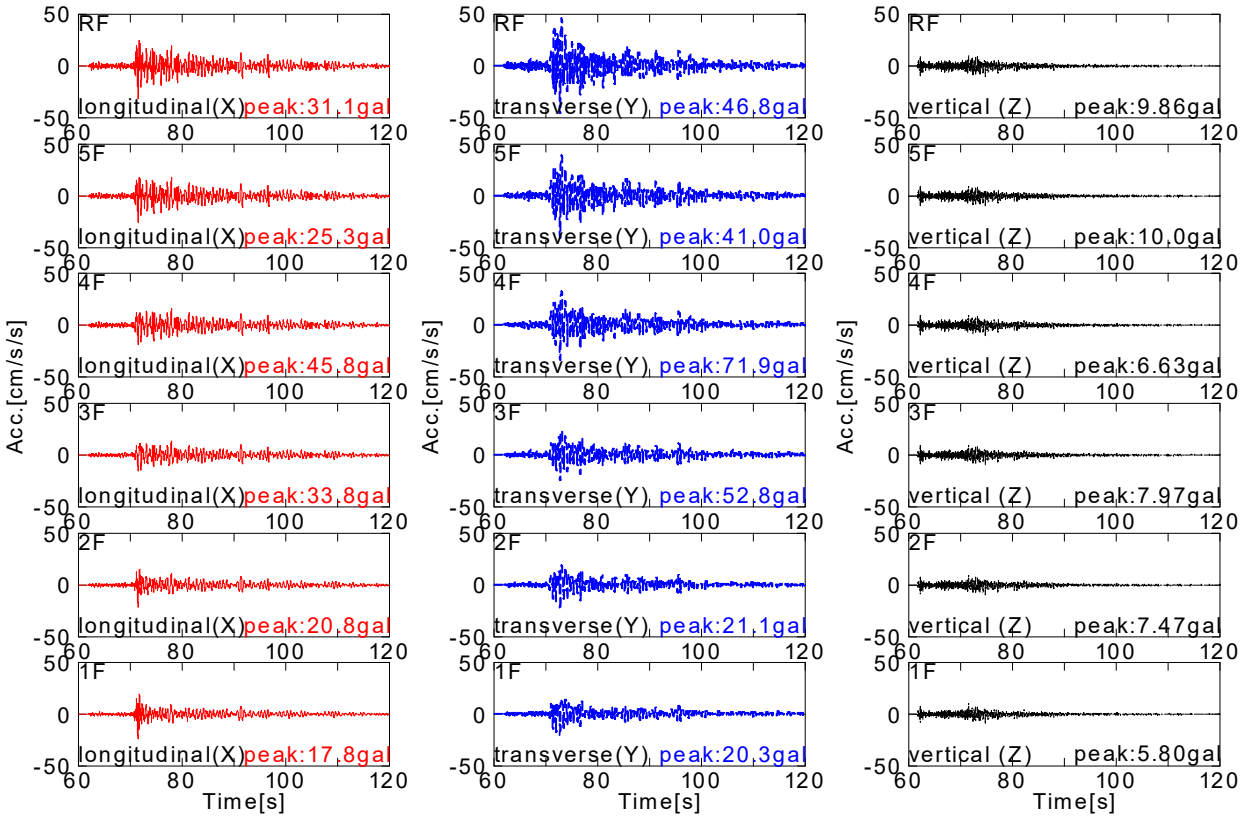

KGU Kanazawa Hakkei Campus No.5 Building (24 June, 2019, 9:12:01 JST,lat.35.322° N, long.139.623° E)

Fig.2 – Observed acceleration waveforms (24 June, 2019 EQ)

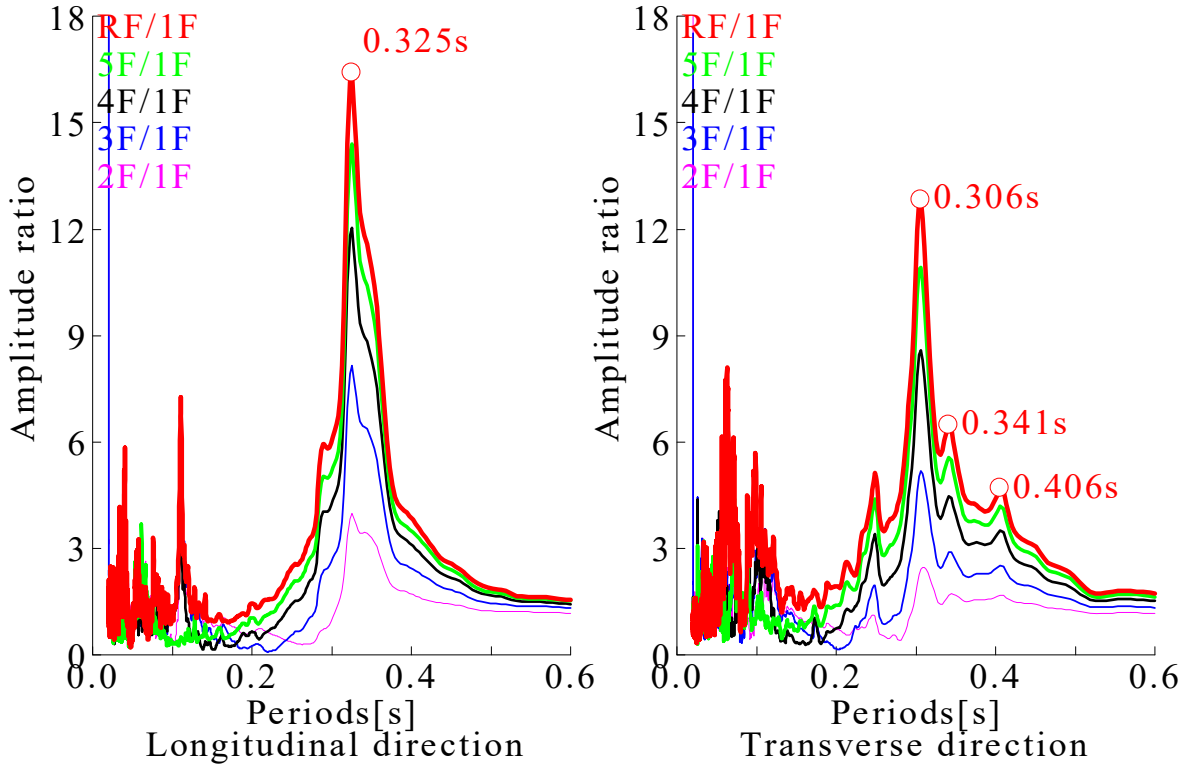

Fig.3 – Fourier spectrum ratios (24 June, 2019 EQ)

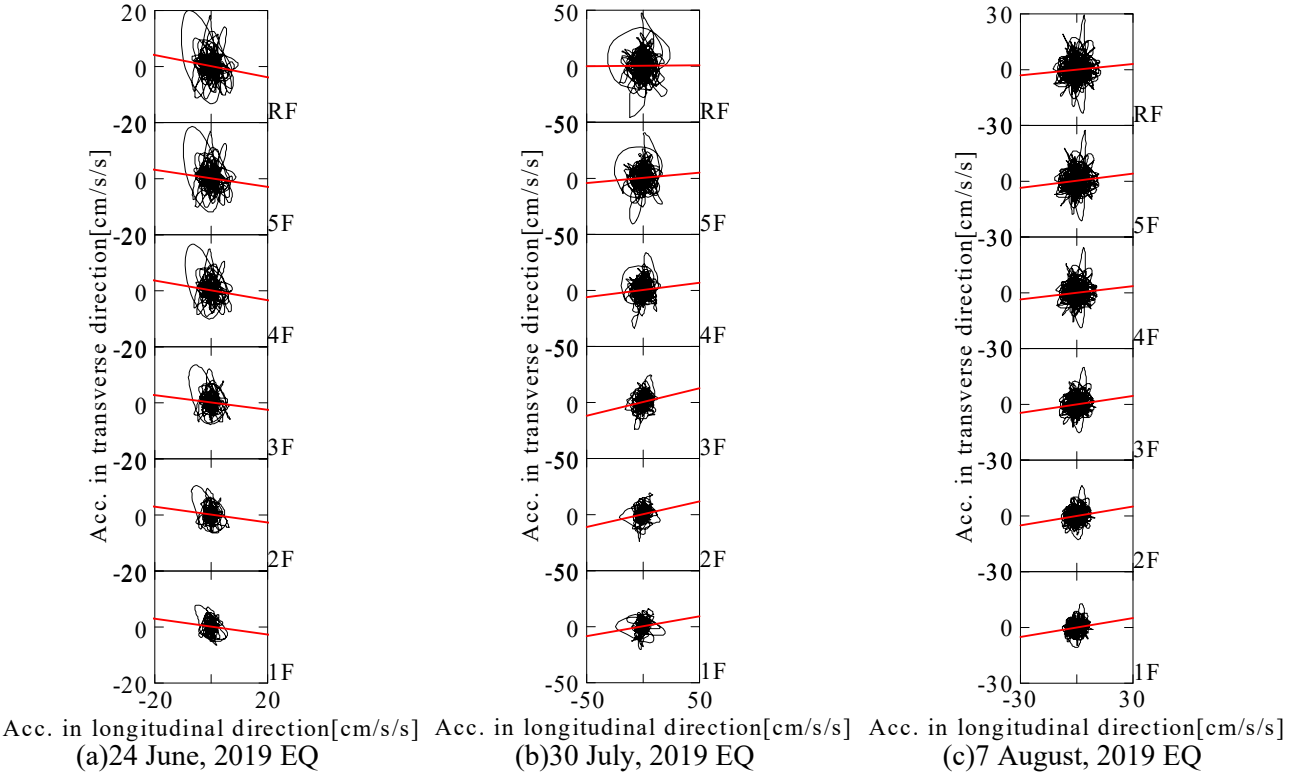

Fig.4 – Acceleration orbits and assumption of a principal axes

4. Analytical results

Fig.5 shows the temporal change of the predominant period from 31 March, 2019 to 6 February, 2020. The maximum of the predominant period was obtained at the X (longitudinal) direction in an earthquake on 17 June, 2019, and at the Y (transverse) direction in an earthquake on 1 February 2020, respectively.

The earthquake on 17 June, 2019, which gave the maximum value of the predominant period in the X (longitudinal) direction, was the earthquake with an hypocenter at an azimuth angle of 32.9°.

The earthquake on 1 February, 2020, which gave the maximum value of the predominant period in the Y (transverse) direction, was the earthquake with an hypocenter at an azimuth angle of 28.8°.

The predominant periods were 0.301 to 0.333 s in the X (longitudinal) direction and 0.281 to 0.308 s in the Y (transverse) direction.

Comparing these minimum and maximum values, they correspond to the change in horizontal stiffness of 82% in the X (longitudinal) direction and 83% in the Y (transverse) direction.

The change in the predominant period was not as great as the change in the period corresponding to the change in stiffness when the columns on the first floor reached yield.

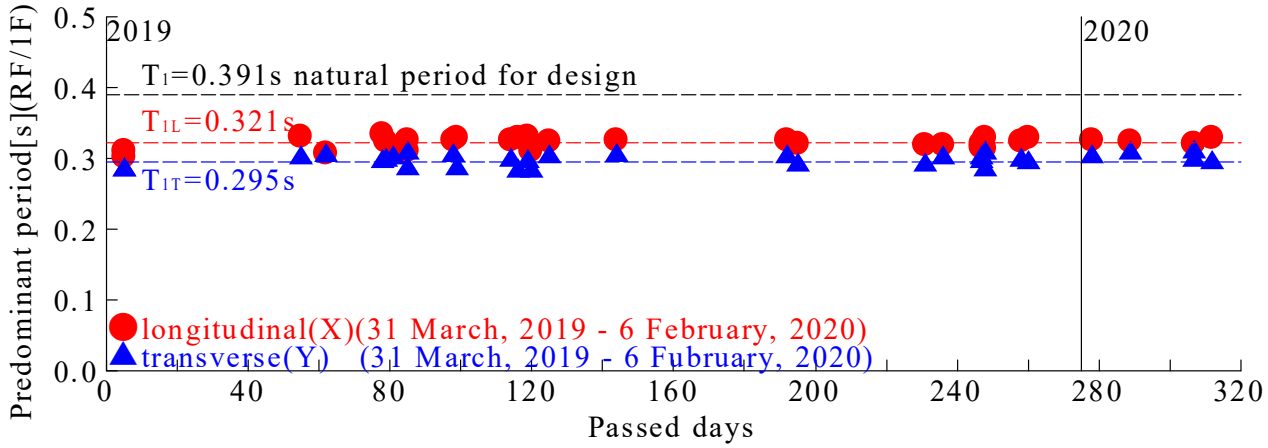

Fig.5 – Change over time in the predominant period (31 March, 2019 – 6 February, 2020)

Fig. 6 shows the relationships among the predominant period and the azimuth angle, the peak maximum response acceleration, and the measured seismic intensity. The peak maximum response acceleration was made dimensionless by dividing by the gravitational acceleration. The same figure shows the following two values; the average value of the ratios of the approximate straight lines in the X (longitudinal) and Y (transverse) directions obtained by the least squares method to the values obtained from the approximate straight lines for the measured values of the predominant period (m) and the coefficient of variation ($C.V.$).

Compared to the other buildings with same height, the Building No.5 has a shorter natural period.

The relationship between the predominant and the maximum acceleration and the measured seismic intensity give the smaller coefficient of variation.

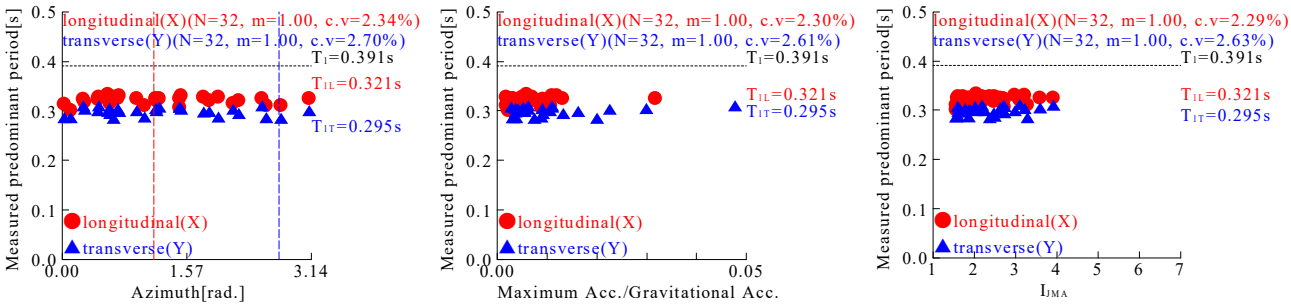

Fig.6 – Relations among the predominant period,
and the Azimuth, and the Maximum Acc./Gravitational Acc., and I_{JMA}
(31 March, 2019 – 6 February, 2020)

Fig. 7 indicates the change over time in the apparent angle of twist θ per unit of length between each measurement floor. The apparent twist angle is not relatively large between RF to 5F on the top, but it is rather relatively large between 4F and 3F.

The maximum value of the apparent twist angle θ in the target building was obtained between 4F and 3F in an earthquake on 12 August, 2019.

The apparent torsion angle per unit length based on the principal axis of acceleration of each floor was distributed within 0.103rad./m.

It can be confirmed from the subsequent earthquake records that no significant increase in the torsional angle occurred.

The examination of the apparent twist angle will be continued in the future.

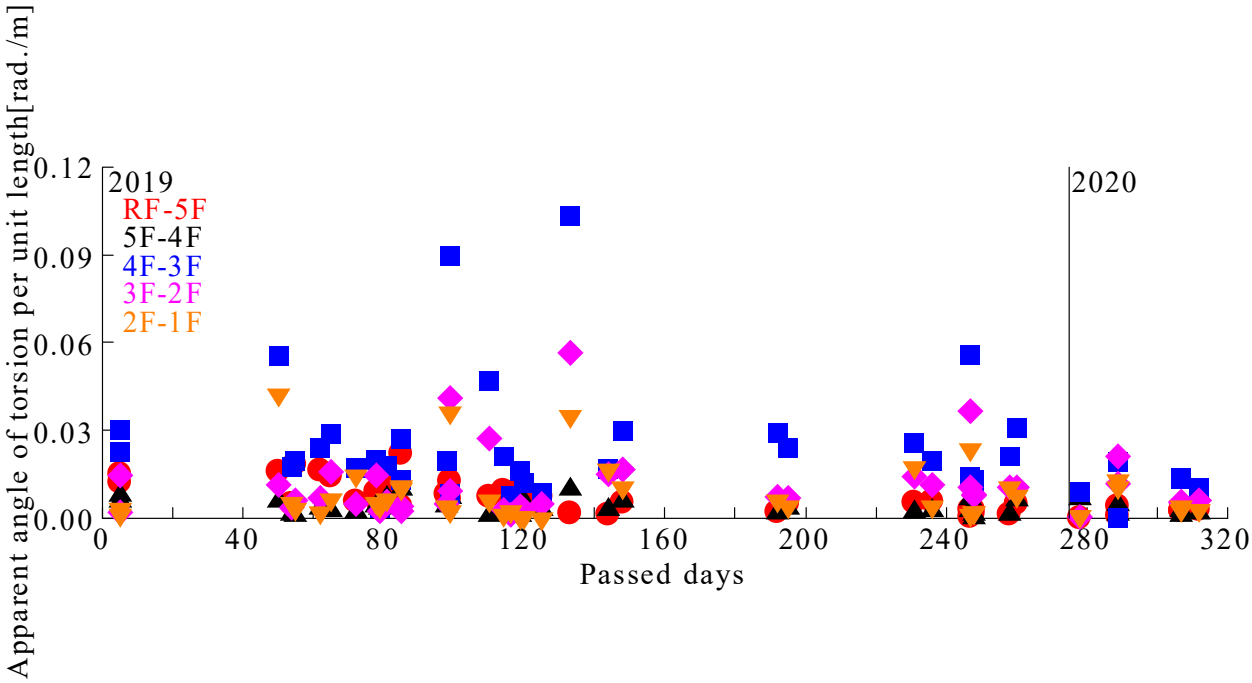

Fig.7 – Change over time in the apparent angle of twist per unit of length
(31 March, 2019 – 6 February, 2020)

Fig.8 indicates the relations among the apparent angle of twist θ per unit length, and the azimuth, and the maximum response acceleration on each floor, and the measured seismic intensity. Here, the maximum response acceleration on each floor is indicated as the sum of vectors in two horizontal directions. No correlation was found between measured seismic intensity and maximum response acceleration and apparent torsion angle compared with the relations between measured seismic intensity and maximum acceleration and the predominant period.

On the other hand, there is a tendency that the apparent torsional angle between 4F and 3F increases in an earthquake with an hypocentral direction at an azimuth angle of 158°. Since there are also azimuthal angles of earthquakes that the building has not experienced, it will be necessary to grasp its behaviors against earthquakes in various azimuths in the future.

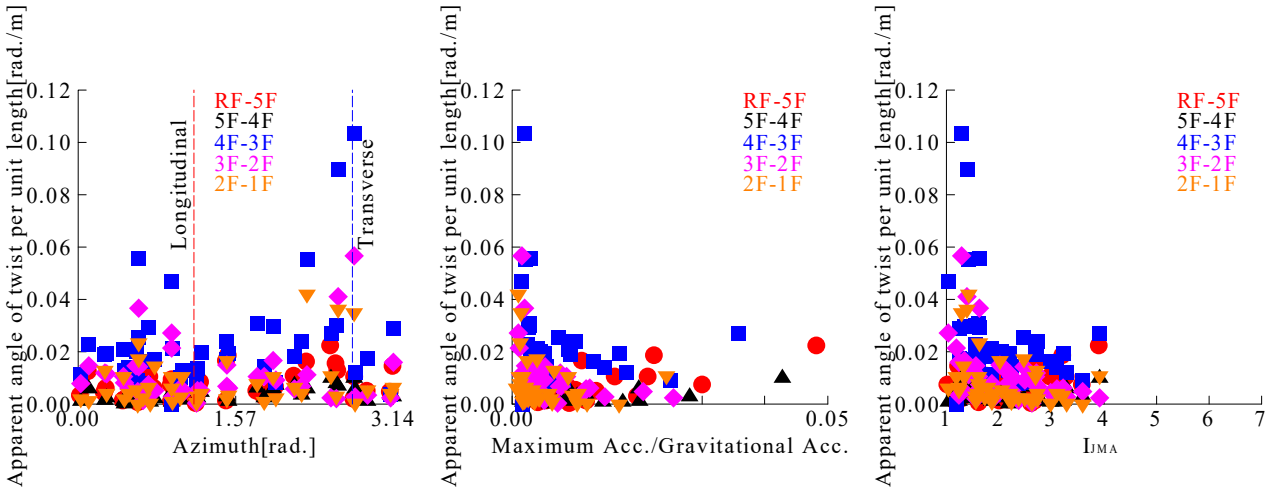

Fig.8 – Relations among the apparent angle of twist per unit of length, and the Azimuth, and the Maximum Acc./Gravitational Acc., and I_{JMA} (31 March, 2019 – 6 February, 2020)

5. Results and Discussion

Compared to the other buildings with same height, the Building No.5 has a shorter natural period. The change in the predominant period was not as great as the change in the period corresponding to the change in stiffness when the columns on the first floor reached yield. The apparent torsion angle per unit length based on the principal axis of acceleration of each floor was distributed within 0.103rad./m.

Further earthquake response of the target building will be examined, taking into consideration aging changes, influences of torsion and other factors in deterioration.

6. Acknowledgements

We wish to express our special thanks to Prof. Emeritus Norio Abeki, Kanto Gakuin University for his valuable advice and comments on the occasion of seismometer installation.

This study was carried out as part of Private University Research Branding Project in Kanto Gakuin University, "Protecting Life and Connecting Hope - Fundamentals of New Disaster Prevention, Disaster Mitigation and Recovery, and Establishment of Core of Excellence".

7. References

[1] Toshinari Ota and Hiroshi Watanabe (2016) “Dynamic Characteristics of a Re-reinforced Steel Reinforced Concrete Building Based on Seismic Observation”, *Proceedings of the 11th International Workshop on Seismic Microzoning and Risk Reduction,* Granada, Spain, 79-86.

[2] Toshinari Ota and Hiroshi Watanabe (2017) “Dynamic Characteristics of a Re-reinforced Steel Reinforced Concrete Building Based on Seismic Observation, --Using observed first natural period and predominant period--”, *The 17th international forum “New Ideas of a New Century, Proceedings of the 17th International Scientific Conference*, 3, Khabarovsk, Russia, 323-328.

[3] Aya Kajiwara, Toshinari Ota and Hiroshi Watanabe (2018) "Preparation of Criteria for Damage on Re-reinforced Steel Reinforced Concrete Building Based on Seismic Observation", *Proceedings of the 12th International Workshop on Seismic Microzoning and Risk Reduction*, Yokohama, Japan, 8pages.

[4] Koichi Kusunoki (2006) "Residual Seismic Capacity Evaluation of Existing Buildings after an Earthquake", *Concrete journal*, 44, 5, 102-105 (in Japanese).

[5] Japan Meteorological Agency (9 February, 2020) "http://www.jma.go.jp/jma/index.html".

[6] Geospatial Information Authority of Japan (9 February, 2020) "https://www.gsi.go.jp/".

